International Journal of Pharmaceutics 379 (2009) 226–234

Contents lists available at ScienceDirect

International Journal of Pharmaceutics

journal homepage: www.elsevier.com/locate/ijpharm

Pharmaceutical Nanotechnology

Development and physicochemical characterization of copper complexes-loaded PLGA nanoparticles

T. Courant[a,b], V.G. Roullin[a,*], C. Cadiou[b], F. Delavoie[c], M. Molinari[d], M.C. Andry[a], F. Chuburu[b,**]

[a] Institut de Chimie Moléculaire de Reims, CNRS UMR 6229, UFR Pharmacie Reims, 51 rue Cognacq-Jay, 51100 Reims, France
[b] Institut de Chimie Moléculaire de Reims, CNRS UMR 6229, UFR des Sciences Exactes et Naturelles, Bâtiment 18 - Europol'Agro, BP 1039, 51687 Reims Cedex 2, France
[c] Laboratoire de Microscopie Electronique Analytique, INSERM UMRS 926, 21 rue Clément Ader, 51685 Reims Cedex 2, France
[d] Laboratoire de Microscopies et d'Etudes des Nanostructures, UFR des Sciences, Université de Reims Champagne-Ardenne, 21 rue Clément Ader, 51685 Reims Cedex 2, France

ARTICLE INFO

Article history:
Received 30 January 2009
Received in revised form 17 March 2009
Accepted 27 March 2009
Available online 5 April 2009

Keywords:
Nanoparticles
Poly(lactide-co-glycolide)
Triacetin
Copper
Double-emulsion

ABSTRACT

PLGA nanoparticles were prepared via a modified W/O/W emulsion solvent diffusion process, in which all formulation components were fully biocompatible and biodegradable. Different independent processing parameters were systematically studied. Nanoparticles were characterized by DLS (particle size, polydispersity, ζ-potential) and TEM/AFM (surface morphology). An optimized formulation was used to encapsulate copper complexes of cyclen and DOTA as potential PET imaging agents. Results showed that the predominant formulation factors appeared to be the lactide-to-glycolide (L:G) ratio of PLGA, the nature of the diffusion phase, and the presence of hydroxyl ions in the first-emulsion aqueous phase. By regulating those 3 parameters, PLGA nanoparticles were prepared with very good preparation yields (>95%), a size less than 200 nm and a polydispersity index less than 0.1. TEM pictures showed nanoparticles with a narrow size distribution, a spherical shape and a smooth surface. The optimized formulation allowed to encapsulate Cu–cyclen and Cu–DOTA complexes with an encapsulation efficiency between 20% and 25%.

1. Introduction

The ability to image molecular events *in vivo* is of great interest to investigate biochemical and physiological processes in living organisms. These goals can be achieved by using specific imaging probes able to target particular tissues or cell types and to monitor diseases even at early development stages. For this purpose, sensitive molecular imaging techniques like the radionuclide based positron emission tomography are undoubtedly among the most sensitive molecular imaging techniques (Ametamey et al., 2008). The PET technique requires the use of positron emitting isotopes linked to the molecule of interest (Miller et al., 2008). Several positron emitting radionuclides exist for incorporation into probes, among which ^{64}Cu. (Heppeler et al., 1999; Yoo et al., 2004). The long half-life of ^{64}Cu is useful for studying biochemical processes with slow pharmacokinetics (Ametamey et al., 2008). This radionuclide is coordinated by a ligand, either a cyclen or a DOTA molecule (Scheme 1), which is able to ensure a strong thermodynamic stability and kinetics inertness for the resulting complex in order to prevent *in vivo* prejudicial demetallation (Bianchi et al., 1991). As previously stated, it is important to deliver the right dose of radioactivity at a given target site. Recently, pharmaceutical formulations have been designed for this purpose, bearing in mind the necessity to improve the therapeutic efficacy while reducing deleterious side effects (Brannon-Peppas and Blanchette, 2004; Maeda et al., 2000). Nano-objects such as liposomes (Hamoudeh et al., 2008) or micelles can be used for this objective. Nanoparticles (NPs) can also be very useful since they offer some specific advantages over liposomes, for instance they help to increase the stability of drugs and possess useful controlled release (CR) properties (Soppimath et al., 2001). Moreover, the size of these objects should allow their diffusion out of the blood vessels to reach the pathological areas. In particular, nanoparticles in the size range of 20–200 nm have been shown to accumulate preferentially at tumor sites through an enhanced permeability retention effect (Jain, 1999).

Several nanomaterials made of various building blocks ranging from conventional lipids to synthetic or natural polymers have been explored. Synthetic polymers and natural macromolecules have been extensively researched as colloidal materials for nanoparticle production design for drug delivery. Synthetic polymers present the advantage of high purity and reproducibility over natural polymers. Research in the biomedical area has extensively focused on the polyester family, i.e. poly(lactic acid) (PLA), poly(ε-caprolactone) (PCL), poly(glycolic acid) (PGA) because of their biocompatibility

* Corresponding author. Tel.: +33 3 26 91 80 54; fax: +33 3 26 91 37 44.
** Corresponding author.
E-mail addresses: gaelle.roullin@univ-reims.fr (V.G. Roullin), francoise.chuburu@univ-reims.fr (F. Chuburu).

0378-5173/$ – see front matter © 2009 Elsevier B.V. All rights reserved.
doi:10.1016/j.ijpharm.2009.03.036

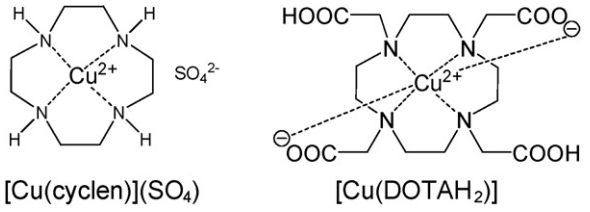

Scheme 1.

and biodegradability properties (Espuelas et al., 1998; Mundargi et al., 2008). In particular, poly(lactide-co-glycolide) (PLGA) is FDA-approved for human use (Brigger et al., 2002; Jain, 2000). PLGA and its various derivatives have set the basis to develop micro- or nanoparticles encapsulating therapeutic drugs for controlled release applications (Bose and Bogner, 2007; Narisawa et al., 1994). Indeed, they present inherent advantages over the conventional devices, such as extended release rates in addition to their biocompatibility/biodegradability and ease of administration via injection.

The preparation of submicron PLGA particles containing an active agent raises serious challenges that do not necessarily exist when preparing larger diameter microparticles. The optimal formulation should satisfy the following: (i) submicron size production with a high recovery yield, (ii) high encapsulation efficiency and bioavailability of the active agent, (iii) minimal 'burst' effect of the effective agent, (iv) low levels of toxic agents used in formulation (excluding active agents) (v) process scalable to large quantities. In practice, it is difficult to satisfy all the aforementioned criteria; compromises usually have to be made in at least one of these conditions when preparing nanoparticles (Birnbaum et al., 2000).

Most nanoparticle formulations are based on preliminary microemulsions (Kwon et al., 2001). They are characterized by a great stability in suspension due to their very small size. This stability is essentially the consequence of significant steric repulsion between droplets (Anton et al., 2008). Common methods used in the preparation of nanoparticles include high-energy emulsification techniques, to create oil-in-water (O/W) and water-in-oil-in-water (W/O/W) emulsions. Furthermore, they allow a good NPs size control and a relative narrow particle size distribution.

In this work, a modified double-emulsion (W/O/W)–solvent diffusion method was developed to encapsulate hydrophilic macrocyclic copper complexes. Since the radio-labelled pharmaceuticals possess the same physicochemical and biochemical properties than the unlabelled compounds, the copper complexes used herein are based on cyclen and DOTA cavities but the metal cation is not radioactive. The preparation and the optimization of the W/O/W method using a non-toxic solvent partially miscible in water, i.e. triacetin (Karlstad et al., 1992) and Poloxamer 188 (Pluronic® F-68) as surfactant agent are reported. The influence of some formulation variables on the nanoparticle characteristics such as polymer composition (lactide/glycolide ratio), polymer concentration in the organic phase, sonication characteristics, composition of the diffusion phase, internal aqueous phase volume, concentration of the stabilizing agent and aqueous phase pH, nature of the encapsulated complex (neutral/ionic, as well as counter-anion influence), have been investigated in order to control and optimize the process. The resulting NPs properties such as mean particle hydrodynamic diameters, surface morphology and drug loading content are also reported.

2. Materials and methods

2.1. Materials

All chemicals were used as received without further purification. Solvents were of reagent grade. Poly(lactide-co-glycolide) (PLGA, 50:50, 65:35, 85:15 lactide/glycolide) were purchased from Sigma–Aldrich, France. Poloxamer 188 (Pluronic® F-68, polyethyleneglycol-co-polypropyleneglycol-co-polyethyleneglycol) was purchased from Sigma-Aldrich France. Water for injections (Ecotainer® - Aqua B. Braun) was used for all batches. 1,2,3-Triacetoxypropane (triacetin) was purchased from Sigma–Aldrich, France. 95% (v/v) ethanol was obtained from Charbonneaux Brabant (France).

2.2. Synthesis of [Cu(cyclen)]SO_4

A methanolic solution of $CuSO_4.6H_2O$ (0.64 mmol, 10 mL) was added dropwise to a solution of cyclen (1,4,7,10-tetraazacyclododecane 0.58 mmol) in methanol (10 mL). The dark blue solution was refluxed and further concentrated by evaporation. The complex could either be obtained in solution in less than 1 h or further precipitated as a dark blue powder by addition of diethyl ether (0.17 g, 88%). The mass spectrum of the powder was recorded with a Q-TOF mass spectrometer (Micromass, Manchester, UK) equipped with an electrospray ionization (ESI) source operated in the positive ion mode.

Elemental Anal. Calc. for $C_8H_{20}N_4CuSO_4$—powder (331.88 g mol^{-1}): C, 28.95; H, 6.07; N, 16.88. Found: C, 29.09; H, 6.10; N, 16.96%. ESI-MS (m/z): calc. for $[Cu(C_8H_{19}N_4)]^+$ 234.1; found 234.1.

2.3. Synthesis of [Cu($DOTAH_2$)]

$DOTAH_4$ (0.20 mmol) and $CuSO_4.6H_2O$ (0.20 mmol) were dissolved in 25 mL of distilled water. Then 3.0 mL of a NaOH solution (0.1 mol L^{-1}) were added (pH = 3.3) and the mixture was left at room temperature. The complex could either be obtained in solution in less than 1 h or as light blue crystals after 3 days.

Elemental Anal. Calc. for $C_{16}H_{26}N_4CuO_8$—crystals (465.95 g mol^{-1}): C, 41.24; H, 5.62; N, 12.02. Found: C, 41.41; H, 5.65; N, 12.07%. ESI-MS (m/z): calc. for $[Cu(C_{16}H_{25}N_4O_8)]^+$ 464.1; found 464.1.

2.4. Nanoparticles preparation

The formation of nanoparticles was achieved by adjusting the multiple emulsion technique, i.e. water (internal, W_i)-in-oil (O)-in water (external, W_e). Batches of nanoparticles were prepared using two types of devices: a high-speed homogenizer (IKA Ultra Turrax® T25) and an ultrasonic probe (Vibracel VC 750). Temperature was maintained at ~20–25 °C during all emulsification steps. The two sonication times were fixed to 30 s, according to sonication times usually reported in the literature (Song et al., 2008) while mechanical emulsification times were set between 2 and 5 min. Ultra Turrax® was used at various homogenization speeds: 8000, 16000 and 24000 rpm. The first-emulsion (W_i/O) was formed by emulsification between an aqueous solution containing various amounts Pluronic® F-68 (0.01–0.1%, w/v) and metal complexes and an organic solution of PLGA in 5 mL triacetin. Then, 10 mL of an aqueous solution containing the same percentage of Pluronic® F-68 (0.01–0.1%, w/v) were added to this primary emulsion to obtain the double-emulsion (W_i/O/W_e). Afterwards, the droplets were converted into nanoparticles through the solvent diffusion step, carried out with addition of 150 mL of hydroalcoholic mixtures for which the composition has been studied. Raw nanoparticle suspensions were obtained within 0.5 h. Subsequently, the hydroalcoholic diffusion phase was replaced by water either by evaporation or by dialysis. Dialysis technique was carried out introducing the colloidal suspension containing the nanoparticles (10 mL) in a dialysis membrane (Spectrum, Spectrapore® 6.0, MWCO 24 kDa); the suspension was dialyzed three times at 20 °C

against 1.8 L of deionised water for at least 2 h under magnetic stirring.

In this study, the influence of some processing parameters and polymer characteristics on NPs mean diameter and polydispersity indexes was evaluated (L:G ratio of PLGA, PLGA concentration, emulsification device, diffusion phase composition, internal aqueous phase volume, surfactant concentration and pH of the internal phase). Unless otherwise mentioned, all the experiments were conducted by varying one of the parameters while keeping all the others at a set of standard conditions. All batches of nanoparticles were produced in triplicate.

2.5. Determination of entrapment efficiencies

The non-encapsulated complexes were separated from the nanoparticles by centrifugation for 1 h at 4 °C at 30,000 g (Beckman Avanti™ 30 Centrifuge, France). Then the supernatant was dosed by UV–vis spectrophotometry (Cary 5000, Varian, France) at 592 and 734 nm for [Cu(cyclen)] SO_4 and [Cu(DOTAH$_2$)] respectively. Repeated washing steps of the NPs sediments with water were performed in order to remove the complexes potentially adsorbed at the NPs surface (washing water volumes = centrifuged suspension volumes). No signal was detected by UV–vis spectrophotometry from the washing solutions, which indicated that no complex adsorption occurred.

Copper complexes entrapment efficiency (EE, %) and drug loading efficiency (DLE, %, w/w) were calculated by Eqs. (1) and (2), respectively:

$$\mathrm{EE} = \frac{\text{mass of copper complex in particles}}{\text{mass of copper complex used in formulation}} \times 100 \quad (1)$$

$$\mathrm{DLE} = \frac{\text{mass of copper complex in particles}}{\text{mass of recovered particles}} \times 100 \quad (2)$$

2.6. Particle size analysis and ζ-potential measurements

Dynamic light scattering (DLS) was used for measurement of average hydrodynamic diameters and polydispersity indexes (PdIs) (Malvern Zetasizer Nano-ZS, Malvern Intruments, UK). Each sample was analyzed in triplicate at 20 °C at a scattering angle of 173°. Pure water was used as a reference dispersing medium.

ζ-potential data were collected through electrophoretic light scattering at 25 °C, 150 V, in triplicate for each sample (Malvern Zetasizer Nano-ZS, Malvern Intruments, UK), in pure water. The instrument was calibrated with a Malvern-50 mV standard before each analysis cycle.

2.7. Morphological studies

The shape and surface morphology of the PLGA NPs were investigated by transmission electron microscopy (TEM) and atomic force microscopy (AFM). A drop of NPs suspension was placed on a 200-mesh copper grid covered with Formvar/carbon. After negative staining with 2% (w/v) uranyl acetate for 1 min, the copper grid was then dried at room temperature before being loaded in the transmission electron microscope (CM30, Philips, Limeil-Brevannes, France) at an accelerating voltage of 250 kV.

Samples for AFM imaging were prepared by placing a drop of PLGA NPs suspension on a freshly cleaved mica sheet and allowing it to dry in the air. AFM imaging was performed using a Nanoscope III (Veeco, Dourdan, France) in tapping mode. A silicon tip with a spring constant of 46 N m^{-1} and a resonant frequency around 300 kHz was used in the study. AFM images were generated with a scan rate of 1 Hz and 256 lines per image. Experiments were performed at constant room temperature. During the scans, proportional and integral gains were increased to the value just below the feedback started to oscillate. Images were processed only by flattening to remove background slopes.

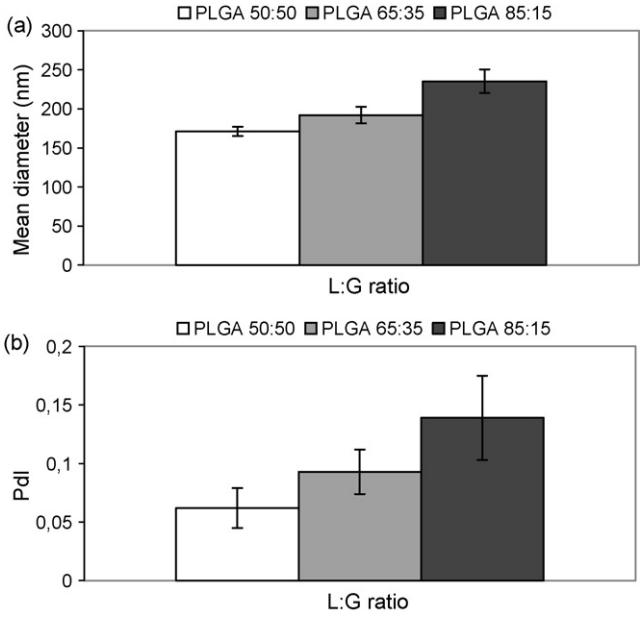

Fig. 1. Effect of L:G ratio on (a) particle mean diameters and (b) corresponding polydispersity indexes, PdIs. Values are presented ±sd (n = 9). PLGA concentration 3% (w/v), F-68 concentration 0.01% (w/v) in both W_i and W_e aqueous phases.

3. Results and discussion

3.1. Effect of preparation variables on nanoparticles characteristics

In order to produce copper-loaded nanoparticles corresponding to a mean diameter less than 200 nm with a narrow size distribution (PdI < 0.1), the influence of several isolated factors on the (W_i/O/W_e) process conditions was analyzed.

3.1.1. Effect of the lactide/glycolide ratio

Three different lactide-to-glycolide ratios (L:G) of PLGA presenting similar molecular weights were used to check the influence of the L:G ratio on mean particle size and PdI. Polymer concentration in the organic phase was fixed to 3% (w/v) and F-68 concentration in both W_i and W_e aqueous phases was fixed to 0.01% (w/v). It can be seen (Fig. 1) that the mean diameters and the PdIs were noticeably affected by the L:G ratio; indeed increasing the L:G ratio increased the mean diameters and the PdIs, as already reported by Lemoine et al. (1996). The mean diameter increased by 60 nm with an increase of ratio from 50:50 to 85:15, giving a mean diameter higher than 200 nm, which is not acceptable for the required *i.v.* applications. In parallel, the PdI increased with the L:G ratio: only PLGA 50:50 allowed to obtain nanoparticles with a narrow size range (PdI < 0.1) since PLGA 65:35 produced a PdI in the 0.1-range and PLGA 85:15 a value higher than 0.1. This increase can be correlated to the polymer cristallinity. As the L:G ratio increases, the better chain organization taking place in lactic crystalline microdomains increases which prevents further chain rearrangements during polymer desolvation; as a result, mean particle diameters increase. Consequently, PLGA 50:50 appeared to be the better choice to obtain nanoparticles with a size less than 200 nm and a PdI less than 0.1.

3.1.2. Effect of PLGA concentration

The PLGA concentration was varied from 1.5% to 8.0% (w/v) while the F-68 concentrations in both W_i and W_e phases remained con-

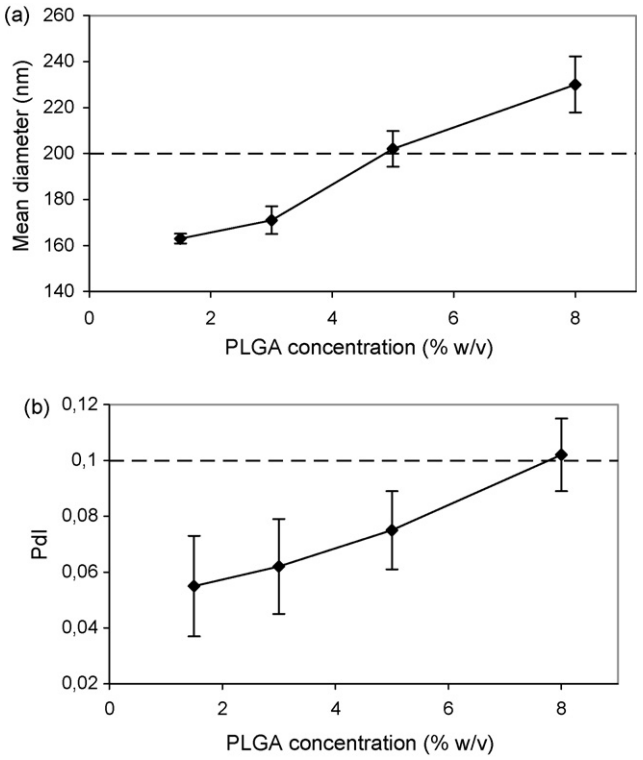

Fig. 2. Effect of PLGA concentration on (a) particle mean diameters and (b) corresponding polydispersity indexes, PdIs. Values are presented ±sd ($n = 9$). F-68 concentration 0.01% (w/v) in both W_i and W_e aqueous phases.

stant and equal to 0.01% (w/v). This surfactant concentration was determined by preliminary experiments which showed that it was sufficient to obtain double-emulsions suitable for nanoparticles production. Fig. 2 shows the effect of the polymer concentration on the mean diameter and the PdI of the resulting nanoparticles. These two parameters increased almost linearly with increasing PLGA concentration, in agreement with the findings of Kwon et al. (2001) and Song et al. (1997), leading to mean diameters higher than 200 nm for PLGA concentrations above 5% (w/v). Nevertheless, the particle size distribution remained narrow (PdI ~ 0.1). Indeed, increasing PLGA concentration leads to an increase of the organic phase viscosity. The consecutive higher viscous resistance to the shear forces induces the formation of droplets with larger sizes and then hinders the nanoparticles formation. Moreover, with the increase of the PLGA amount, the chosen F-68 quantity was probably insufficient to correctly stabilize the emulsion, and then to inhibit the droplets coalescence during the solvent diffusion step (Kwon et al., 2001 and *vide infra*). Consequently, a polymer concentration of 3% (w/v) for a 0.01% (w/v) F-68 concentration was a good compromise (i) to produce NPs with satisfactory mean diameters and PdIs and (ii) to bring sufficient PLGA amounts to efficiently entrap active molecules.

3.1.3. Influence of the high energy emulsification parameters

Batches of nanoparticles using PLGA 50:50, 3% (w/v)/triacetin/F-68 0.01% (w/v) were prepared using a high-speed homogenizer or an ultrasonic probe. With the high-speed homogenizer, polydisperse NPs distributions, with size ranges between 500 nm and 1 μm, were obtained. The mean diameters tended to be smaller with an increase of the homogenization speed but polydispersity could not be avoided (Abismail et al., 1999; Anton et al., 2008). Ultrasonic probes are known to be more powerful devices which theoretically allow the formation of smaller emulsions and subsequent smaller nanoparticles. When using this kind of probe, a single population of nanoparticles was obtained. Sonication power appeared to have a quite negligible influence until the value of 22 W (32% amplitude). Beyond this value, it seemed that the additional energy was too high and destabilized the system since the distribution became polydisperse. The difference observed between these two devices is their dispersive energy mechanisms. In the case of high-speed homogenizer, most of the provided energy is dissipated and lost in viscous frictions (Friberg and Jones, 1994; Walstra, 1993), the remaining energy being insufficient to overcome the huge interfacial surface energy of nanoemulsions. On the contrary, sonication locally brings sufficient energy to overcome this drawback, enabling the formation of emulsions. The droplets are subsequently stabilized by the presence of surfactant molecules which further favourably contribute to the interfacial tension reduction (Behrend et al., 2000).

3.1.4. Influence of the diffusion phase composition

One of the most important factors influencing the NPs size is the solvent diffusion step. The mechanism of nanoparticle formation based on emulsion template was previously described (Choi et al., 2002; Kwon et al., 2001). They proposed that the solvent solution is dispersed in the continuous phase as globules. The stability of this emulsion is enhanced by the presence of stabilizing agent molecules adsorbed at the interface. The subsequent addition of the diffusion phase destabilizes this equilibrium and triggers the solvent diffusion to the continuous phase. During the migration of the solvent molecules, new nanometric globules are produced from the microdroplets and gradually become poorer in solvent. As a result, the polymer chains in the globules precipitate at the contact with the continuous non-solvent phase. An increase in the globule diffusion rate should lead to the formation of smaller and monodisperse nanoparticles. This kinetics can be related to the value of the globule diffusion coefficient into the continuous phase, which is described by the Stokes–Einstein equation:

$$D = \frac{kT}{6\pi r\eta}, \tag{3}$$

where D ($cm^2\ s^{-1}$) is diffusion coefficient, k ($1.3805 \times 10^{-23}\ J\ K^{-1}$) is the Boltzman constant, T (K) is the temperature, r is the globule hydrodynamic volume radius and η (cP) is the diffusion phase viscosity. In order to enhance the diffusion rate to obtain smaller NPs, the variables to be adjusted are the temperature T and the viscosity of diffusion phase η. Since PLGA has a low glass-transition temperature (between 30 and 40 °C, Astete and Sabliov, 2006), a temperature superior to 30 °C is unsuitable. Indeed, exceeding the glass-transition temperature would lead to "melted" PLGA with physicochemical properties unsuitable for formulation applications. Consequently, formulation temperature was fixed at 20 °C. Concerning the aqueous diffusion phase, its viscosity can be modified through the addition of co-solvents, such as alcohols. For biocompatibility reasons, ethanol was chosen as co-solvent, which also allows to improve the triacetin solubility (miscible in ethanol whatever the proportions and 1 in 14 (v/v) in water, Palmieri, 2006). Hydroalcoholic diffusion phases of various compositions were tested to modulate the triacetin diffusion and therefore the NPs final size. Polymer concentration in the organic phase was fixed to 3% (w/v) and F-68 concentration in both W_i and W_e aqueous phases was fixed to 0.01% (w/v). Fig. 3 shows the influence of the composition of the hydroalcoholic diffusion phase on the mean diameters and PdIs of the NPs. It can be noticed that the NPs size increased dramatically for a water percentage superior to 50% (v/v). Moreover, for aqueous percentages above 70% (v/v), several populations were observed. The smaller sizes and values of PdI were obtained for a 5% (v/v) water diffusion phase. These results indicate that as expected, one of the major factors to be controlled is the diffusion kinetics, the triacetin diffusion being more rapid with

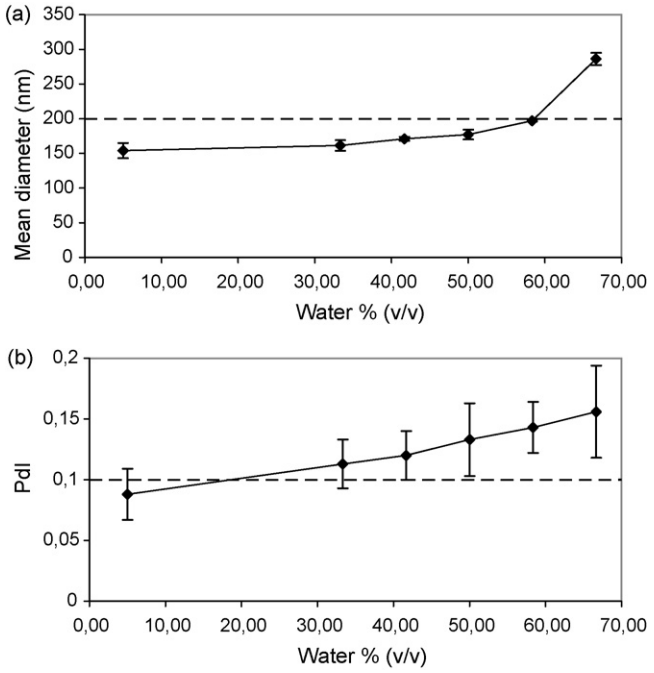

Fig. 3. Influence of the water percentage in the hydroalcoholic diffusion phase on (a) particle mean diameters and (b) corresponding PdI values. Values are presented ±sd ($n = 9$). PLGA concentration 3% (w/v), F-68 concentration 0.01% (w/v) in both W_i and W_e aqueous phases.

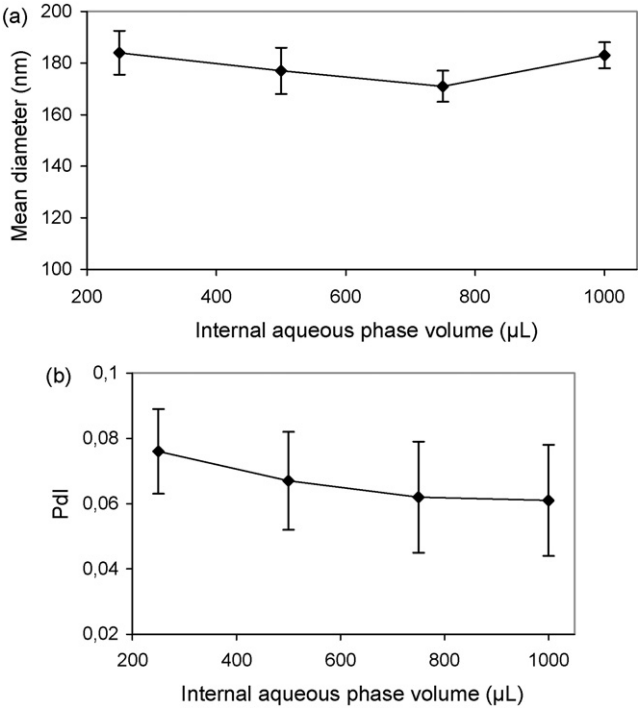

Fig. 4. Influence of the internal aqueous phase (W_i) volume on (a) particle mean diameters and (b) corresponding PdI values. Values are presented ±sd ($n = 9$). PLGA concentration 3% (w/v), F-68 concentration 0.01% (w/v) in both W_i and W_e aqueous phases.

95% (v/v) ethanol diffusion phase. As a result, the synthesized NPs exhibited satisfying mean diameters (~160 nm) and PdIs (<0.1).

3.1.5. Influence of the internal aqueous phase volume

The effect of the W_i phase volume was also explored while keeping organic phase volume identical (5 mL). Polymer concentration in the organic phase was fixed to 3% (w/v) and F-68 concentration in both W_i and W_e aqueous phases was fixed to 0.01% (w/v). Fig. 4 shows that the influence of an increase of W_i volume from 250 µL to 1 mL was quite negligible since the particle sizes remained in the 160–180 nm range and the PdI was less than 0.1. These results agree well with Ngaboni Okassa et al. (2005) and Zambaux et al. (1998) experiments, concerning the preparation of PLA nanoparticles for which a threefold increase of the W_i volume phase led to particles with equivalent NPs size characteristics. Moreover and as mentioned by these authors, it should be noted that an increase in the W_i phase volume could lead to an increase of the NPs loading.

3.1.6. Concentration of Pluronic® F-68 surfactant

Surfactant concentrations in W_i and W_e phases of 0.01 and 0.1% (w/v) were alternatively used to evaluate the effect of F-68 concentration on the NPs size (Table 1) while keeping the PLGA concentration fixed to 3% (w/v). First, a 10-fold increase of F-68 percentage in W_i for a constant F-68 percentage in W_e of 0.01% resulted in the reduction of both mean diameters and PdIs (entries 1 and 2). It is likely that a higher F-68 presence in W_i resulted in a more regular and stable first-emulsion which in turn provided smaller droplets and allowed, in the consecutive step, the formation of smaller NPs. For the same F-68 percentages in W_i, the increase of F-68 concentration in W_e (entries 1 and 3 or 2 and 4) did not result in reducing the NPs size. These findings are not in agreement with some previously reported ones (Quintanar-Guerrero et al., 1996; Zambaux et al., 1998) where the increase of the surfactant concentrations in W_e led to smaller particles. This discrepancy can herein be explained by the fact that, in the studied ternary system (PLGA/triacetin/F-68 water), the increase of F-68 in W_e slows down the triacetin diffusion into the hydroalcohic phases. Actually, introducing 0.1% (w/v) F-68 in the aqueous phase of a triacetin/water (1/4, v/v) emulsion resulted into increasing the demixing time from 4 h to over a week. Thus, F-68 presence in W_e could result in slower triacetin diffusion rate, subsequent slower polymer precipitation, which would allow more nanodroplet coalescence to occur, finally producing larger NPs. From mean diameters and PdIs point of view, the best results were obtained for 0.1% and 0.01% (w/v) F-68 concentrations in W_i and W_e phases respectively (Table 1 entry 2).

3.1.7. Influence of the pH in the internal phase (W_i)

This factor was evaluated since it may play a role in entrapment efficiency of drugs (Song et al., 1997) whose hydrosolubility is pH-dependent (for instance, $CuDOTAH_2$). Polymer concentration in the organic phase was fixed to 3% (w/v) and F-68 concentration in both W_i and W_e aqueous phases was fixed to 0.01% (w/v). As seen in Fig. 5, the mean diameter was strongly reduced with increasing pH (from 171 nm at pH = 7 to 109 nm at pH = 13) while PdI was maintained at a value <0.1 all over the pH range. The reduction of the particle size consecutive to the pH evolution has already been observed by Quintanar-Guerrero et al. (1996) for PLA nanoparticles using F-68 as a surfactant. These results were attributed to the presence of hydroxyl ions at the oil-water interface since Marinova et al. (1996) indeed suggested that the adsorption of

Table 1
Influence of F-68 concentration on NPs mean diameters and PdIs.

Entries	F-68% (w/v) in W_i	F-68% (w/v) in W_e	Mean diameter (nm)	PdI (±sd)
1	0.01	0.01	197 ± 3 nm	0.075 ± 0.014
2	0.1	0.01	168 ± 2 nm	0.061 ± 0.014
3	0.01	0.1	209 ± 2 nm	0.062 ± 0.027
4	0.1	0.1	211 ± 3 nm	0.042 ± 0.029

PLGA concentration 3% (w/v).

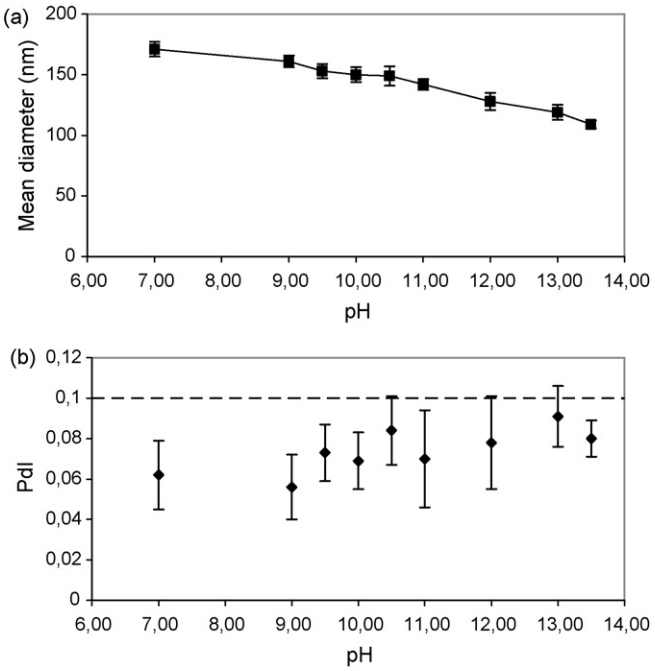

Fig. 5. Influence of the internal aqueous phase (W_i) pH on (a) particle mean diameters and (b) corresponding PdI values. Values are presented ±sd ($n = 9$). PLGA concentration 3% (w/v), F-68 concentration 0.01% (w/v) in both W_i and W_e aqueous phases.

hydroxyl ions was an inherent property of the oil–water interface. Moreover Beattie and Djerdev (2004) suggested that the hydroxyl ions adsorption could be reinforced in the presence of surfactant molecules, OH^- ions being stabilized through hydrogen bonds by the oxygen atoms of the polyoxyethylene chains of the non-ionic surfactant (Beattie and Djerdev, 2004; Becher and Schick, 1987). To point out the role of OH^- ions in our system, we prepared some F-68 water/triacetin emulsions in presence of various electrolytes in the W_i aqueous phase (Table 2). In presence of hydroxyl ions, the emulsions appeared to be more stable than those prepared in presence of sulphate or chloride anions (entries 1–2 versus 3–5), which corroborated our hypothesis. Furthermore, it is likely that the cations play an important part in the system stabilisation since with K^+ and Bu_4N^+, the corresponding emulsions and NPs suspensions were less stable than with Na^+ (entries 4–5 versus 3). In fact, it was previously pointed out that PEG chains tended to coordinate Na^+, due to the Lewis base character of PEG chains (Ratner and Shriver, 1988). So, when introducing in the system both Na^+ and OH^- ions, the stabilizing mechanisms should largely counterbalance the destabilizing ones which generally occur during O/W interface formation. Ultimately, the presence of OH^- in solution produces a decrease in the F-68 hydration (Collins and Washabaugh, 1985; Hofmeister, 1888; Lopez-Leon et al., 2003; Vadnere et al., 1984) thereby improving packing at the interface and thus reducing the nanodroplet size. Finally, in Table 2, the indicated sizes correspond to the NPs suspensions once they were centrifuged and dialyzed to remove flocculates and solvating ions. The best formulation results were indeed obtained for NaOH (entry 3), since it allowed reduced particle sizes and PdIs, a production yield recovery well above 95% and a maximal stability from 4 °C to room temperature.

3.2. Optimal PLGA-NPs preparation and morphological characterization

From the abovementioned experiments, W_i phase pH was adjusted through NaOH concentration; its value resulted from a compromise between the smallest mean diameters (Fig. 5) and a pH which can avoid accelerated polyester degradation. Furthermore, the presence of NaOH allowed a maximal recovery in NPs production (>95%). Consequently, the pH of W_i in the optimized formulation was maintained equal to 10.

The optimal formulation results, in terms of size characteristics and morphology, were obtained for the following settings: 750 μL of 0.1% (w/v) F-68 pH 10 aqueous solution (W_i) were emulsified in 5 mL triacetin (O) containing 150 mg PLGA 50:50 for 30 s, 32% ampl. (22 W), subsequently similarly sonicated in 10 mL 0.01% (w/v) F-68 aqueous solution (W_e). NPs were precipitated by addition of 150 mL 95% (v/v) ethanol. NPs prepared with this optimal formulation exhibited a mean diameter of 154.0 ± 5.1 nm ($n = 9$). The PdI values (0.069 ± 0.014, $n = 9$) indicated a very narrow size distribution. These results are very interesting, compared to what is usually reported for similar ternary systems generated by W/O/W process for which PdIs are usually higher (from 0.15 to 0.4) (Gryparis et al., 2007; Kocbek et al., 2007; Ngaboni Okassa et al., 2007; Yin et al., 2006).

The DLS measurements of the three independently produced batches were not appreciably different from each other (Table 3). This accounted for the robustness and reproducibility of the procedure and the ternary system suitability. TEM and AFM pictures (Fig. 6a and b) showed NPs with a spherical shape and a smooth

Table 2
Influence of W_i salts presence on emulsion stability and NPs characteristics.

Entries	Cation	Anion	Emulsion stability[a]	Production efficiency[b]	NPs suspension stability	NPs mean diameter (nm, ±sd)	PdI (±sd)
1	Na^+	SO_4^{2-}	1	1	Unstable (sedimentation in 24 h)	258 ± 2	0.116 ± 0.026
2	Na^+	Cl^-	1	Aggregates no NPs	–	–	–
3	Na^+	OH^-	3	3	Very stable (several months)	150 ± 6	0.069 ± 0.014
4	K^+	OH^-	2	2	Unstable (flocculation in 48 h)	177 ± 3	0.079 ± 0.006
5	Bu_4N^+	OH^-	2	2	Unstable (flocculation in 48 h)	214 ± 5	0.099 ± 0.016

PLGA concentration 3% (w/v), F-68 concentration 0.01% (w/v) in both W_i and W_e aqueous phases.
[a] 0: Immediate demixtion after the end of the stirring; 1: stability < 3 min; 2: 3 min < stability < 10 min; 3: stability > 10 min.
[b] 1: Estimated production yield < 50%; 50% < estimated production yield < 95%; 3: estimated production yield > 95%.

Table 3
Raw mean diameters and PdIs of optimized blank NPs.

Raw data	Batch 1			Batch 2			Batch 3		
	1	2	3	1	2	3	1	2	3
Mean diameter (nm)	152	155	156	149	148	147	158	157	161
PdI	0.064	0.051	0.075	0.076	0.079	0.053	0.055	0.097	0.057
ζ-potential	−52.0	−50.2	−46.5	−47.7	−49.0	−49.7	−46.7	−48.3	−49.6

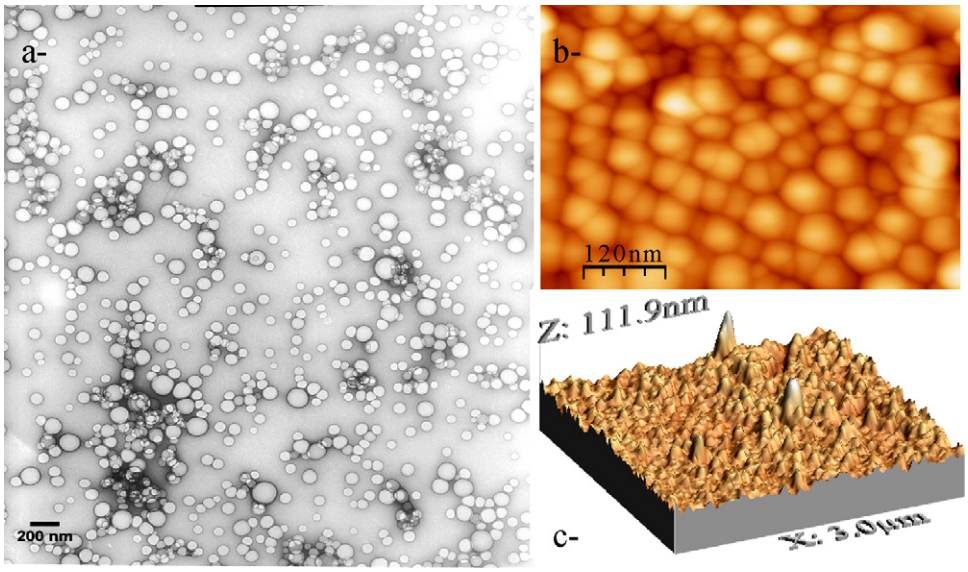

Fig. 6. (a) TEM photographs of nanoparticles prepared from PLGA; bar corresponded to 200 nm. (b) Surface topography and (c) corresponding 3-D AFM-images of NPs obtained by tapping-mode AFM and visualized in amplitude mode.

Table 4
Raw mean diameters and PdIs of copper complexes-loaded NPs.

Raw data	Batch 1			Batch 2			Batch 3		
	1	2	3	1	2	3	1	2	3
Cu(cyclen)-NPs									
Mean diameter (nm)	183	174	185	188	194	189	184	184	186
PdI	0.072	0.076	0.079	0.024	0.057	0.062	0.070	0.041	0.064
ζ-potential	−43.4	−47.7	−48.8	−42.2	−43.7	−43.7	−45.3	−46.5	−47.2
Cu(DOTA)-NPs									
Mean diameter (nm)	104	102	103	116	117	117	120	120	127
PdI	0.097	0.089	0.095	0.109	0.081	0.106	0.091	0.100	0.099
ζ-potential	−47.0	−49.5	−49.3	−42.9	−43.1	−43.8	−46.2	−47.8	−49.4

surface; on AFM 3-D reconstructed images, the mean diameter could be evaluated about 112 nm (Fig. 6c). The differences observed between the two morphological evaluations were essentially due to the fact that, in DLS, the hydrodynamic radius of the particle (which takes into account the double solvation layer) is measured. On the contrary, TEM and AFM were performed on dried, dialyzed NPs, i.e. depleted of surface ions, solvent and non-solvent molecules. Consequently, the genuine mean diameter (by TEM) is generally far smaller that the hydrodynamic one (by DLS) (Zanetti-Ramos et al., 2009). The ζ-potential of NPs after dialysis was found strongly negative (-48.9 ± 1.8 mV, $n = 9$), whereas ζ-potential of raw (undialyzed) suspensions displayed values of -24.2 ± 1.1 mV. This discrepancy demonstrated efficient F-68 adsorption at the nanoparticles surface. This coating afforded good stability to the nanoparticles suspension and contributed to conceal polymer carboxylic charges, which could be a great advantage to prevent *in vivo* NPs opsonization (Santander-Ortega et al., 2006).

3.3. Copper complexes encapsulation—influence of the complex nature

The optimized formulation (in terms of mean diameters and PdIs) was used to encapsulate two macrocyclic copper complexes [Cu(cyclen)](SO_4) and [$CuDOTAH_2$] (Scheme 1) in times compatible with the ^{64}Cu half-life (less than two hours for both complex and subsequent nanoparticle preparation). Both complexes enabled to obtain spherical nanoparticles. By comparison with the production yields obtained with blank NPs, the production yields remained unchanged with the incorporation of [$CuDOTAH_2$] complex (estimated >95%) whereas it slightly decreased with the incorporation of [Cu(cyclen)](SO_4). NPs presented mean hydrodynamic diameters of 185.0 ± 5.3 nm for particles containing the cationic $[Cu(cyclen)]^{2+}$ complex[1] and $113{,}0 \pm 9{,}0$ nm for particles containing $[CuDOTA]^{2-}$ (since pH 10 for W_i induced an ionisation of [$CuDOTAH_2$]) (Table 4). PdIs were 0.061 ± 0.018 and 0.096 ± 0.009 respectively. By comparison with the blank NPs mean sizes (154.0 ± 5.1 nm), the complexes encapsulation resulted in a 35-nm size increase for $[Cu(cyclen)]^{2+}$ and a 40-nm size decrease for $[CuDOTA]^{2-}$. These variations could not be attributed to a macrocyclic template effect since, in this case, both complexes would induce an increase in the NPs size. These results (size and NPs recovery) can nevertheless be understood as following: (i) the crucial presence of hydroxyl ions enabled, as aforementioned, the droplets stabilization, the subsequent NPs size reduction (compatible with the therapeutic targets) and improved recovery yields; (ii) when kosmotropic SO_4^{2-} ions (Collins and Washabaugh, 1985; Hofmeister, 1888; Iwanaga et al., 1998; Lopez-Leon et al., 2003; Vadnere et al., 1984) were present as counterions of $[Cu(cyclen)]^{2+}$, they partially counter-balanced the favourable influence of OH^- and led to an increase in the measured NPs sizes. Besides, in the case of $[CuDOTA]^{2-}$ encapsulation, at basic pH the complex exhibited two anionic carboxylate arms which could behave like hydroxyl ions; they would hence be stabilized through hydrogen bonds by the oxygen atoms of the polyoxyethylene chains

[1] Since for this complex, sulphate is a non coordinating anion, the complex is named $[Cu(cyclen)]^{2+}$.

of the non-ionic surfactant and lead to the reduction of the particle size.

The ζ-potentials of dialyzed copper-loaded NPs were found to be identical for both complexes (-45.4 ± 2.26 mV for $[Cu(cyclen)]^{2+}$-NPs and -46.6 ± 2.71 mV for $[CuDOTA]^{2-}$ NPs). No significant change could be observed between ζ-potentials of blank NPs (Table 3) and NPs containing copper complexes (Table 4). This may signify that copper complexes are not adsorbed at the NPs surface, otherwise the ζ-potential values would have been affected.

By comparison with the production yields obtained with blank NPs, the production yields remained unchanged with the incorporation of $[CuDOTAH_2]$ complex (estimated >95%) whereas it slightly decreased with the incorporation of $[Cu(cyclen)](SO_4)$. Encapsulation efficiencies (EE) were 26% for $[Cu(cyclen)](SO_4)$ and 19% for $[CuDOTAH_2]$. The calculated drug loading efficiencies (DLE) were 3.0% and 2.7% for $[Cu(cyclen)](SO_4)$ and $[CuDOTAH_2]$, respectively. These results compared well with those reported by (Gryparis et al., 2007) for which the double-emulsion method led to cisplatin encapsulation in same yield range.

4. Conclusion

In this work, we reported a modified W/O/W process to obtain copper complexes effective loading into PLGA nanoparticles. These optimized nanoparticles were spherical, monodisperse, with a mean diameter well below 200 nm, reaching 110 nm in the case of $[CuDOTAH_2]$ complex encapsulation. We showed that the simultaneous presence of hydroxyl ions, Na^+ and PEG segments of the F-68 surfactant molecules in the first-emulsion aqueous phase resulted in a highly structured droplet formation and ensuing remarkably small nanoparticles. On the basis of these results, as well as the relatively good encapsulation efficiencies, the currently described nanoparticles might represent a promising formulation as PET imaging agents. This easy-to-run method could be extended to the synthesis of radiolabelled complex-loaded nanoparticles in a sterile way while keeping production times and operating procedures compatible with the 12.7 h half-life of ^{64}Cu. Further experiments are presently on-going to assess this point, as well as the nanoparticle *in vivo* behaviour. Co-encapsulation of various hydrophilic drugs will subsequently be tested, in order to design multimodal imaging NPs.

Acknowledgement

Thomas Courant acknowledges a doctoral fellowship from la Région Champagne-Ardenne.

References

Abismail, B., Canselier, J.P., Wilhelm, A.M., Delmas, H., Gourdon, C., 1999. Emulsification by ultrasound: drop size distribution and stability. Ultrason. Sonochem. 6, 75–83.

Anton, N., Benoit, J.P., Saulnier, P., 2008. Design and production of nanoparticles formulated from nanoemulsion templates—a review. J. Control. Release 128, 185–189.

Ametamey, S.M., Honer, M., Schubiger, P.A., 2008. Molecular imaging with PET. Chem. Rev. 128, 1501–1516.

Astete, C.E., Sabliov, C.M., 2006. Synthesis and characterization of PLGA nanoparticles. J. Biomater. Sci. Polym. Ed. 17 (3), 247–289.

Beattie, J.K., Djerdev, A.M., 2004. The pristine oil/water interface: surfactant-free hydroxide-charged emulsions. Angew. Chem. 116, 3652–3655.

Becher, P., Schick, M.J., 1987. In: Schick, M.J. (Ed.), Nonionic Surfactants; Surfactant Science Series 23. Marcel Dekker, New York, pp. 435–491.

Behrend, O., Ax, K., Schubert, H., 2000. Influence of continuous phase viscosity on emulsification by ultrasound. Ultrason. Sonochem. 7, 77–85.

Bianchi, A., Micheloni, M., Paoletti, P., 1991. Thermodynamic aspects of the polyaazacycloalkane complexes with cations and anions. Coord. Chem. Rev. 110, 17–113.

Birnbaum, D.T., Kosmala, J.D., Brannon-Peppas, L., 2000. Optimization of Preparation Techniques for poly(lactic acid-co-glycolic acid) Nanoparticles. J. Nanopart. Res. 2, 173–181.

Bose, S., Bogner, R.H., 2007. Solventless pharmaceutical coating processes: a review. Pharm. Dev. Technol. 12, 115–131.

Brannon-Peppas, L., Blanchette, J.O., 2004. Nanoparticle and targeted systems for cancer therapy. Adv. Drug Deliv. Rev. 56, 1649–1659.

Brigger, I., Dubernet, C., Couvreur, P., 2002. Nanoparticles in cancer therapy and diagnosis. Adv. Drug Deliv. Rev. 54, 631–651.

Choi, S.-W., Kwon, H.-Y., Kim, W.-S., Kim, J.-H., 2002. Thermodynamic parameters on poly(d,l-lactide-co-glycolide) particle size in emulsification–diffusion process. Colloids Surf. A: Physicochem. Eng. Aspects 201, 283–289.

Collins, K.D., Washabaugh, M.W., 1985. The Hofmeister effect and the behaviour of water at interfaces. Q. Rev. Biophys. 18, 323–422.

Espuelas, M.S., Legrand, P., Cheron, M., Barratt, G., Puisieux, F., Renedo, M.J., Devissaguet, J.P., Irache, J.M., 1998. Interaction of amphotericin B with polymeric colloids: 2. Effect of poloxamer on the adsorption of amphotericin B onto poly(e-caprolactone) nanospheres. Colloids Surf. B: Biointerfaces 11, 203–212.

Friberg, S.E., Jones, S., 1994. In: Kroschwith, J.I. (Ed.), Kirk-Othmer Encyclopedia of Chemical Technology, 9. Wiley, New York, pp. 393–413.

Gryparis, E.C., Hatziapostolou, M., Papadimitriou, E., Avgoustakis, K., 2007. Anticancer activity of cisplatin-loaded PLGA-mPEG nanoparticles on LNCaP prostate cancer cells. Eur. J. Pharm. Biopharm. 67, 1–8.

Hamoudeh, M., Kamleh, M.A., Diab, R., Fessi, H., 2008. Radionuclides delivery systems for nuclear imaging and radiotherapy of cancer. Adv. Drug Deliv. Rev. 60, 1329–1346.

Heppeler, A., Froidevaux, S., Macke, H.R., Jermann, E., Béhé, M., Powell, P., Hennig, H., 1999. Radiometal-labelled macrocyclic chelator-derivatised somatostatin analogue with superb tumor targeting properties and potential for receptor-mediated internal radiotherapy. Chem. Eur. J. 5, 1974–1981.

Hofmeister, F., 1888. Zur Lehre von der Wirkung der Salze. Naunyn-Schmiedebergs Arch. Exp. Pathol. Pharmak. 24, 247–260.

Iwanaga, T., Suzuki, M., Kunieda, H., 1998. Effect of added salts or polyols on the liquid crystalline structures of polyoxyethylene-type non-ionic surfactants. Langmuir 14, 5775–5781.

Jain, R.K., 1999. Transport of molecules, particles, and cells in solid tumors. Annu. Rev. Biomed. Eng. 1, 241–243.

Jain, R.A., 2000. The manufacturing techniques of various drug loaded biodegradable poly(lactide-co-glycolide) (PLGA) devices. Biomaterials 21, 2475–2490.

Karlstad, M.D., Killefer, J.A., Bailey, J.W., DeMichele, S.J., 1992. Parenteral nutrition with short- and long-chain triglycerides: triacetin reduces atrophy of small and large bowel mucosa and improves protein metabolism in burned rats. Am. J. Clin. Nutr. 55, 1005–1011.

Kocbek, P., Obermajer, N., Cegnar, M., Kos, J., Kristl, J., 2007. Targeting cancer cells using PLGA nanoparticles surface modified with monoclonal antibody. J. Control. Release 120, 18–26.

Kwon, H.-Y., Lee, J.-Y., Choi, S.-W., Jang, Y., Kim, J.-H., 2001. Preparation of PLGA nanoparticles containing estrogen by emulsification–diffusion method. Colloids Surf. A: Physicochem. Eng. Aspects 182, 123–130.

Lemoine, D., Francois, C., Kedzierewicz, F., Preat, V., Hoffman, M., Maincent, P., 1996. Stability study of nanoparticles of poly(epsilon-caprolactone), poly(d,l-lactide) and poly(d,l-lactide-co-glycolide). Biomaterials 17, 2191–2197.

Lopez-Leon, T., Jodar-Reyes, A.B., Bastos-Gonzalez, D., Ortega-Vinuesa, J.L., 2003. Effects in the stability and electrophoretic mobility of polystyrene latex particles. J. Phys. Chem. B 107, 5696–5708.

Maeda, H., Wu, J., Sawa, T., Matsumura, Y., Hori, K., 2000. Tumor vascular permeability and the EPR effect in macromolecular therapeutics: a review. J. Control. Release 65, 271–284.

Marinova, K.G., Alargova, R.G., Denkov, N.D., Velev, O.D., Petsev, D.N., Ivanov, I.B., Borwankar, R.P., 1996. Charging of oil-water interfaces due to spontaneous adsorption of hydroxyl ions. Langmuir 12, 2045–2051.

Miller, P.W., Long, N.J., Vilar, R., Gee, A.D., 2008. Synthesis of ^{11}C, ^{18}F, ^{15}O, and ^{13}N radiolabels for positron emission tomography. Angew. Chem. Int. Ed. 47, 8998–9033.

Mundargi, R.C., Babu, V.R., Rangaswamy, V., Patel, P., Aminabhavi, T.M., 2008. Nano/micro technologies for delivering macromolecular therapeutics using poly(d,l-lactide-co-glycolide) and its derivatives. J. Control. Release 125, 193–209.

Narisawa, S., Nagata, M., Danyoshi, L., Yoshino, H., Murata, K., Hirakawa, Y., Noda, K., 1994. An organic acid-induced sigmoidal release system for oral controlled-release preparations. Pharm. Res. 11, 111–116.

Ngaboni Okassa, L., Marchais, H., Douziech-Eyrolles, L., Cohen-Jonathan, S., Soucé, M., Dubois, P., Chourpa, I., 2005. Development and characterization of sub-micron poly(d,l-lactide-co-glycolide) particles loaded with magnetite/maghemite nanoparticles. Int. J. Pharm. 302, 187–196.

Ngaboni Okassa, L., Marchais, H., Douziech-Eyrolles, L., Hervé, K., Cohen-Jonathan, S., Munnier, E., Soucé, M., Linassier, C., Dubois, P., Chourpa, I., 2007. Optimization of iron oxide nanoparticles encapsulation within poly(d,l-lactide-co-glycolide) sub-micron particles. Eur. J. Pharm. Biopharm. 67, 31–38.

Palmieri, A., 2006. Handbook of Pharmaceutical Excipients. In: Rowe, R.C., Sheskey, P.J., Owen, S.C. (Eds.), fifth ed., London, pp. 790-791.

Quintanar-Guerrero, D., Fessi, H., Allémann, E., Doelker, E., 1996. Influence of stabilizing agents and preparative variables on the formation of poly(d,l-lactic acid) nanoparticles by an emulsification–diffusion technique. Int. J. Pharm. 143, 133–141.

Ratner, M.A., Shriver, D.F., 1988. Ion transport in solvent-free polymers. Chem. Rev. 88, 109–124.

Santander-Ortega, M.J., Jódar-Reyes, A.B., Csaba, N., Bastos-González, D., Ortega-Vinuesa, J.L., 2006. Colloidal stability of Pluronic F68-coated PLGA nanoparticles: a variety of stabilisation mechanisms. J. Colloid Interface Sci. 302, 522–529.

Song, C.X., Labhasetwar, V., Murphy, H., Qu, X., Humphrey, W.R., Shebuski, R.J., Levy, R.J., 1997. Formulation and characterization of biodegradable nanoparticles for intravascular local drug delivery. J. Control. Release 43, 197–212.

Song, X., Zhao, Y., Wu, W., Bi, Y., Cai, Z., Chen, Q., Li, Y., Hou, S., 2008. PLGA nanoparticles simultaneously loaded with vincristine sulfate and verapamil hydrochloride: systematic study of particle size and drug entrapment efficiency. Int. J. Pharm. 350, 320–329.

Soppimath, K.S., Aminabhavi, T.M., Kulkarni, A.R., Rudzinski, W.E., 2001. Biodegradable polymeric nanoparticles as drug delivery devices. J. Control. Release 70, 1–20.

Vadnere, M., Amidon, G., Lindenbaum, S., Haslam, J.L., 1984. Thermodynamic studies on the gel-sol transition of some Pluronic polyols. Int. J. Pharm. 22, 207–218.

Walstra, P., 1993. Principles of emulsion formation. Chem. Eng. Sci. 48, 333.

Yin, Y., Chen, D., Qiao, M., Lu, Z., Hu, H., 2006. Preparation and evaluation of lectin-conjugated PLGA nanoparticles for oral delivery of thymopentin. J. Control. Release 116, 337–345.

Yoo, J., Reichert, D.E., Welch, M.J., 2004. Comparative *in vivo* behavior studies of cyclen-based copper-64 complexes: regioselective synthesis, X-ray Structure, radiochemistry, log *P*, and biodistribution. J. Med. Chem. 47, 6625–6637.

Zambaux, M.F., Bonneaux, F., Gref, R., Maincent, P., Dellacherie, E., Alonso, M.J., Labrude, P., Vigneron, C., 1998. Influence of experimental parameters on the characteristics of poly(lactic acid) nanoparticles prepared by a double-emulsion method. J. Control. Release 50, 31–40.

Zanetti-Ramos, B.G., Fritzen-Garcia, M.B., de Oliveira, C.S., Avelino Pasa, A., Soldi, V., Borsali, R., Creczynski-Pasa, T.B., 2009. Dynamic light scattering and atomic force microscopy techniques for size determination of polyurethane nanoparticles. Mater. Sci. Eng. C 29, 638–640.